Journal of Applied Mathematics and Computation, 2022, 6(1), 161-166
https://www.hillpublisher.com/journals/JAMC/
ISSN Online: 2576-0653
ISSN Print: 2576-0645

Research on Powered Phase Guidance Method of Ballistic Missile Based on MPSP

Xinsan Li*, Qiang Shen, Can Li, Lixin Wang

Xi'an High-tech Institution, Xi'an, Shaanxi Province, China.

How to cite this paper: Xinsan Li, Qiang Shen, Can Li, Lixin Wang. (2022) Research on Powered Phase Guidance Method of Ballistic Missile Based on MPSP. *Journal of Applied Mathematics and Computation*, 6(1), 161-166.
DOI: 10.26855/jamc.2022.03.017

Received: February 18, 2022
Accepted: March 15, 2022
Published: April 2, 2022

***Corresponding author:** Xinsan Li, Xi'an High-tech Institution, Xi'an, Shaanxi Province, China.
Email: xinsan_2006@163.com

Abstract

Aiming at the trajectory design of ballistic missile in the powered phase, considering the influence of time deviation at the end time, the predictive static programming (MPSP) guidance method under the condition of free end time is deduced in this paper. Aiming at the free and fixed end time. Both flight time and control quantity are closed loop. The amplitude of controls at different times can be adjusted by adjusting the weight coefficient c_f and weight matrix $\boldsymbol{R}_k$ in the performance function. The MPSP guidance method for the powered phase is simulated and analyzed to verify the effectiveness of the free end time MPSP guidance method. The deviation of the flight path angle is in the range of 0.1 deg, and the altitude deviation is in the range of 1.0 m.

Keywords

Guidance, Ballistic, Model Prediction

1. Introduction

The traditional ballistic missile flies to the target stably and accurately according to the preset trajectory. In the traditional sense, the trajectory is divided into two parts: the controlled powered phase and the uncontrolled passive phase [1, 2]. According to whether it is affected by aerodynamics, the passive phase trajectory can be divided into the free flight phase not affected by aerodynamics and the reentry phase affected by aerodynamics. One of the problems in trajectory design is the selection of flight scheme and flight procedure. The selection of flight procedure is closely related to the change law of control variables in each trajectory. Therefore, flight procedure is essentially to explore the change law of control variables with time. Generally, there are two methods of trajectory design, namely, optimal trajectory design method and engineering design method. The optimal trajectory method uses the maximum (or minimum) principle to solve the two-point boundary value problem and obtain the optimal or suboptimal trajectory that meets the requirements of performance index and terminal conditions [3, 4]. Engineering design law is to find the approximate functional relationship of control variables according to the control variables obtained by maximum theory and work practice experience. The trajectory is designed by adjusting the control variables and numerical integration. Obviously, the optimal trajectory design method can obtain the optimal trajectory solution. However, the calculation is very complex and the calculation workload is particularly large [5, 6].

MPSP theory has been applied to aircraft reentry guidance, cruise missile midcourse guidance and terminal guidance with angle constraints [7, 8]. This paper mainly studies the guidance method of tactical ballistic missile based on the model prediction static planning guidance theory.

2. MPSP Guidance Method

For general nonlinear systems, the discrete state equations and output equations are as follows:

$$\boldsymbol{X}_{k+1} = \boldsymbol{F}_k(\boldsymbol{X}_k, \boldsymbol{U}_k) \tag{1}$$

$$\boldsymbol{Y}_k = \boldsymbol{h}(\boldsymbol{X}_k) \tag{2}$$

Where, states $\boldsymbol{X} \in \boldsymbol{R}^n$, controls $\boldsymbol{U} \in \boldsymbol{R}^m$, outputs $\boldsymbol{Y} \in \boldsymbol{R}^p$. The goal of MPSP guidance method is to find out the appropriate controls, so that the actual outputs $\boldsymbol{Y}_N$ and the expected output $\boldsymbol{Y}_N^*$ meet: $\boldsymbol{Y}_N \to \boldsymbol{Y}_N^*$ at the end time.

$$d\boldsymbol{Y}_N = \boldsymbol{A}d\boldsymbol{X}_1 + \boldsymbol{B}d\boldsymbol{U}_1 + \ldots + \boldsymbol{B}_{N-1}d\boldsymbol{U}_{N-1} \tag{3}$$

Where,

$$\boldsymbol{A} = \left[\frac{\partial \boldsymbol{Y}_N}{\partial \boldsymbol{X}_N}\right]\left[\frac{\partial \boldsymbol{F}_{N-1}}{\partial \boldsymbol{X}_{N-1}}\right]\cdots\left[\frac{\partial \boldsymbol{F}_1}{\partial \boldsymbol{X}_1}\right] \tag{4}$$

The expression of the sensitivity matrix between the terminal outputs and the controls is:

$$\boldsymbol{B}_k = \left[\frac{\partial \boldsymbol{Y}_N}{\partial \boldsymbol{X}_N}\right]\left[\frac{\partial \boldsymbol{F}_{N-1}}{\partial \boldsymbol{X}_{N-1}}\right]\cdots\left[\frac{\partial \boldsymbol{F}_{k+1}}{\partial \boldsymbol{X}_{k+1}}\right]\left[\frac{\partial \boldsymbol{F}_k}{\partial \boldsymbol{U}_k}\right] \tag{5}$$

$$k = 1, \ldots, N-1$$

The performance functional is as follows:

$$J = \frac{1}{2}\sum_{k=1}^{N-1}(\boldsymbol{U}_k^0 - d\boldsymbol{U}_k)^T \boldsymbol{R}_k (\boldsymbol{U}_k^0 - d\boldsymbol{U}_k) \tag{6}$$

Where, $\boldsymbol{U}_k^0$ is the current control command, $d\boldsymbol{U}_k$ is the corresponding control command deviation, and $\boldsymbol{R}_k$ is the weight matrix. The control deviation corresponding to step k is:

$$d\boldsymbol{U}_k = -\boldsymbol{R}_k^{-1}\boldsymbol{B}_k^T\boldsymbol{A}_\lambda^{-1}(d\boldsymbol{Y}_N - \boldsymbol{b}_\lambda) + \boldsymbol{U}_k^0 \tag{7}$$

The controls updated in step k are:

$$\boldsymbol{U}_k = \boldsymbol{U}_k^0 - d\boldsymbol{U}_k = \boldsymbol{R}_k^{-1}\boldsymbol{B}_k^T\boldsymbol{A}_\lambda^{-1}(d\boldsymbol{Y}_N - \boldsymbol{b}_\lambda) \tag{8}$$

Where,

$$\boldsymbol{A}_\lambda = \left[-\sum_{k=1}^{N-1}\boldsymbol{B}_k\boldsymbol{R}_k^{-1}\boldsymbol{B}_k^T\right] \tag{9}$$

$$\boldsymbol{b}_\lambda = \left[\sum_{k=1}^{N-1}\boldsymbol{B}_k\boldsymbol{U}_k^0\right] \tag{10}$$

3. Principle of MPSP Guidance at Free Terminal Time

Considering the influence of time deviation Δt_f at the end of time, the influence of higher-order term is ignored after Taylor series expansion of output deviation at the end of time, including:

$$\Delta\boldsymbol{Y}_N = d\boldsymbol{Y}_N + \dot{\boldsymbol{Y}}_N\Delta t_f = \left[\frac{\partial \boldsymbol{Y}_N}{\partial \boldsymbol{X}_N}\right]d\boldsymbol{X}_N + \left[\frac{\partial \boldsymbol{Y}_N}{\partial \boldsymbol{X}_N}\right]\dot{\boldsymbol{X}}_N\Delta t_f = \left[\frac{\partial \boldsymbol{Y}_N}{\partial \boldsymbol{X}_N}\right]d\boldsymbol{X}_N + \left[\frac{\partial \boldsymbol{Y}_N}{\partial \boldsymbol{X}_N}\right]f\left(\boldsymbol{X}_N, \boldsymbol{U}_N\right)\Delta t_f \tag{11}$$

Where, Δt_f is the time deviation relative to the end time t_f, and $\dot{\boldsymbol{X}}_N$ is the state equation corresponding to the discrete-time node N at the end time, assuming $\boldsymbol{U}_N = \boldsymbol{U}_{N-1}$. We can get:

$$\Delta\boldsymbol{Y}_N = d\boldsymbol{Y}_N + \dot{\boldsymbol{Y}}_N\Delta t_f = \sum_{k=1}^{N-1}\boldsymbol{B}_k d\boldsymbol{U}_k + \left[\frac{\partial \boldsymbol{Y}_N}{\partial \boldsymbol{X}_N}\right]\boldsymbol{f}\left(\boldsymbol{X}_N, \boldsymbol{U}_N\right)\Delta t_f \tag{12}$$

Consider the following performance functional:

$$J = \frac{1}{2} c_f \left(\Delta t_f \right)^2 + \frac{1}{2} \sum_{k=1}^{N-1} (\boldsymbol{U}_k^0 - d\boldsymbol{U}_k)^T \boldsymbol{R}_k (\boldsymbol{U}_k^0 - d\boldsymbol{U}_k) \tag{13}$$

In the above formula, c_f is the time deviation coefficient at the end time. Equations (12) and (13) constitute a static optimization problem. The generalized performance functional is:

$$\bar{J} = \frac{1}{2} c_f \left(\Delta t_f \right)^2 + \frac{1}{2} \sum_{k=1}^{N-1} (\boldsymbol{U}_k^0 - d\boldsymbol{U}_k)^T \boldsymbol{R}_k (\boldsymbol{U}_k^0 - d\boldsymbol{U}_k) + \boldsymbol{\lambda}^T \left(\Delta \boldsymbol{Y}_N - \sum_{k=1}^{N-1} \boldsymbol{B}_k d\boldsymbol{U}_k - \left[\frac{\partial \boldsymbol{Y}_N}{\partial \boldsymbol{X}_N} \right] \boldsymbol{f}\left(\boldsymbol{X}_N, \boldsymbol{U}_N \right) \Delta t_f \right) \tag{14}$$

Using the optimization theory, the following results are obtained:

$$\frac{\partial \bar{J}}{\partial d\boldsymbol{U}_k} = -\boldsymbol{R}_k d\boldsymbol{U}_k \boldsymbol{\lambda} + \boldsymbol{U}_k^0 - \boldsymbol{B}_k^T \quad = 0 \tag{15}$$

$$\frac{\partial \bar{J}}{\partial \left(\Delta t_f \right)} = c_f \left(\Delta t_f \right) - \left(\left[\frac{\partial \boldsymbol{Y}_N}{\partial \boldsymbol{X}_N} \right] \boldsymbol{f}\left(\boldsymbol{X} \boldsymbol{\lambda}_N, \boldsymbol{U}_N \right) \right)^T \quad = 0 \tag{16}$$

$$\frac{\partial \bar{J}}{\partial \boldsymbol{\lambda} \boldsymbol{X}} = \Delta \boldsymbol{Y}_N - \left(\sum_{k=1}^{N-1} \boldsymbol{B}_k d\boldsymbol{U}_k + \left[\frac{\partial \boldsymbol{Y}_N}{\partial \quad _N} \right] \boldsymbol{f}\left(\boldsymbol{X}_N, \boldsymbol{U}_N \right) \Delta t_f \right) = 0 \tag{17}$$

From equation (15):

$$d\boldsymbol{U}_k = \left(\boldsymbol{R}_k \right)^{-1} \boldsymbol{B}_k^T \boldsymbol{\lambda} + \boldsymbol{U}_k^0 \tag{18}$$

From equation (16):

$$\Delta t_f = \left(c_f \right)^{-1} \left(\left[\frac{\partial \boldsymbol{Y}_N}{\partial \boldsymbol{X}_N} \right] \boldsymbol{f}\left(\boldsymbol{X} \boldsymbol{\lambda}_N, \boldsymbol{U}_N \right) \right)^T \tag{19}$$

Substituting equation (18) and equation (19) into equation (12), we get:

$$\begin{aligned} \Delta \boldsymbol{Y}_N &= -\left(-\sum_{k=1}^{N-1} \boldsymbol{B}_k \left(\boldsymbol{R}_k \right)^{-1} \boldsymbol{B}_k^T \right) \boldsymbol{\lambda} + \sum_{k=1}^{N-1} \boldsymbol{B}_k \boldsymbol{U}_k^0 + \left[\frac{\partial \boldsymbol{Y}_N}{\partial \boldsymbol{X}_N} \right] \boldsymbol{f}\left(\boldsymbol{X}_N, \boldsymbol{U}_N \right) \Delta t_f \\ &= -\left(-\sum_{k=1}^{N-1} \boldsymbol{B}_k \left(\boldsymbol{R}_k \right)^{-1} \boldsymbol{B}_k^T \right) \boldsymbol{\lambda} + \sum_{k=1}^{N-1} \boldsymbol{B}_k \boldsymbol{U}_k^0 + \\ &\left[\frac{\partial \boldsymbol{Y}_N}{\partial \boldsymbol{X}_N} \right] \boldsymbol{f}\left(\boldsymbol{X}_N, \boldsymbol{U}_N \right) \left(c_f \right)^{-1} \left(\left[\frac{\partial \boldsymbol{Y}_N}{\partial \boldsymbol{X}_N} \right] \boldsymbol{f}\left(\boldsymbol{X}_N, \boldsymbol{U}_N \right) \right)^T \boldsymbol{\lambda} \end{aligned} \tag{20}$$

Among them,

$$\boldsymbol{A}_\lambda = -\sum_{k=1}^{N-1} \boldsymbol{B}_k \left(\boldsymbol{R}_k \right)^{-1} \boldsymbol{B}_k^T \tag{21}$$

$$\boldsymbol{b}_\lambda = \sum_{k=1}^{N-1} \boldsymbol{B}_k \boldsymbol{U}_k^0 \tag{22}$$

$$\boldsymbol{C}_\lambda = \left[\frac{\partial \boldsymbol{Y}_N}{\partial \boldsymbol{X}_N} \right] \boldsymbol{f}\left(\boldsymbol{X}_N, \boldsymbol{U}_N \right) \left(c_f \right)^{-1} \left(\left[\frac{\partial \boldsymbol{Y}_N}{\partial \boldsymbol{X}_N} \right] \boldsymbol{f}\left(\boldsymbol{X}_N, \boldsymbol{U}_N \right) \right)^T \tag{23}$$

Equation (20) can be written as follows:

$$\Delta \boldsymbol{Y}_N = -\boldsymbol{A}_\lambda \boldsymbol{\lambda} + \boldsymbol{b}_\lambda + \boldsymbol{C}_\lambda \boldsymbol{\lambda} \tag{24}$$

From equation (24):

$$\boldsymbol{\lambda} = -\left(\boldsymbol{A}_{\lambda} - \boldsymbol{C}_{\lambda}\right)^{-1}\left(\Delta \boldsymbol{Y}_N - \boldsymbol{b}_{\lambda}\right) \tag{25}$$

Combining formula (19) and formula (25), we can get:

$$\Delta t_f = -\left(c_f\right)^{-1}\left(\left[\frac{\partial \boldsymbol{Y}_N}{\partial \boldsymbol{X}_N}\right]\boldsymbol{f}\left(\boldsymbol{X}_N, \boldsymbol{U}_N\right)\right)^T\left(\boldsymbol{A}_{\lambda} - \boldsymbol{C}_{\lambda}\right)^{-1}\left(\Delta \boldsymbol{Y}_N - \boldsymbol{b}_{\lambda}\right) \tag{26}$$

The updated flight time is:

$$t = t^0 - \Delta t_f = t^0 + \left(c_f\right)^{-1}\left(\left[\frac{\partial \boldsymbol{Y}_N}{\partial \boldsymbol{X}_N}\right]\boldsymbol{f}\left(\boldsymbol{X}_N, \boldsymbol{U}_N\right)\right)^T\left(\boldsymbol{A}_{\lambda} - \boldsymbol{C}_{\lambda}\right)^{-1}\left(\Delta \boldsymbol{Y}_N - \boldsymbol{b}_{\lambda}\right) \tag{27}$$

The updated controls are:

$$\boldsymbol{U}_k = \boldsymbol{U}_k^0 - d\boldsymbol{U}_k = \boldsymbol{R}_k^{-1}\boldsymbol{B}_k^T\left(\boldsymbol{A}_{\lambda} - \boldsymbol{C}_{\lambda}\right)^{-1}\left(\Delta \boldsymbol{Y}_N - \boldsymbol{b}_{\lambda}\right) \tag{28}$$

Equations (27) and (28) are updated flight time and controls respectively. Both flight time and control quantity are closed loop. The amplitude of controls at different times can be adjusted by adjusting the weight coefficient c_f and weight matrix $\boldsymbol{R}_k$ in the performance function.

4. Simulation Analysis

It is assumed that the initial height of the missile after vertical ejection is 10.0m and the initial speed is 10.0m/s. It is required that at the end of the powered phase, the ballistic inclination angle of the missile is 0.0deg, the ballistic deflection angle is 0.0deg, and the flight altitude of the missile is 15000.0m, which meets the initial state conditions of near space flight in the middle section.

The initial controls are guessed through proportional guidance. When the end time is fixed and the time deviation Δt_f of the end time is not considered, the end output can converge to the given error range after 4 iterations. When the end time deviation is freely considered at the end time, the end output can converge to the given error range after 8 iterations. The simulation results are shown in Figures 1-5. When the terminal time is free and fixed, the flight time of the missile is 67.36s and 43.85s respectively. When considering the influence of Δt_f, the flight time of the missile increases by 23.51 s. Figure 1 shows the change curve of normal acceleration command a_z, considering the end time deviation, the normal acceleration command a_z will quickly approach zero. Figure 2 shows the change curve of missile speed V_m. Figure 3 shows the variation curve of Flight path angle γ_m. Due to the constraint on the trajectory inclination at the end time, the angle deviation at the end time is within 0.1 deg. Figure 4 and Figure 5 show the change curve of missile displacement. At the end of the active section, the missile height z_m tends to the constraint value of 15000.0m, and the height deviation can be controlled within 1.0m. The simulation results show that the MPSP guidance method can well meet the requirements of terminal time constraint when the terminal time deviation is considered and not considered in the powered phase of ballistic missile. The flight time of the missile increases when considering the time deviation, and the normal acceleration command a_z will quickly approach zero.

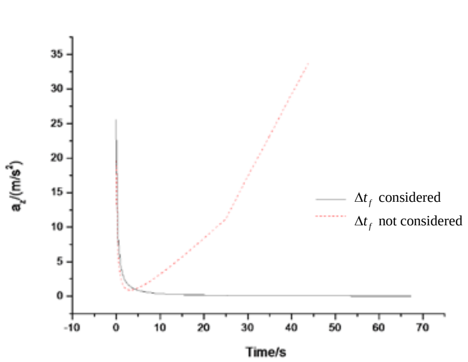

Figure 1. Normal acceleration command change curve.

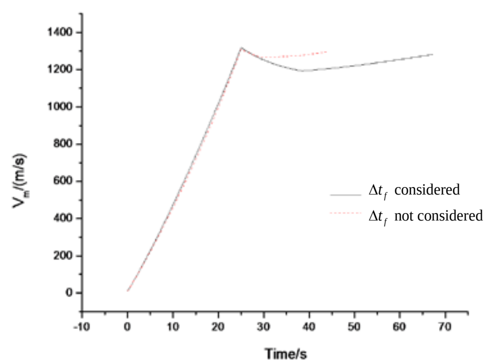

Figure 2. Speed change curve.

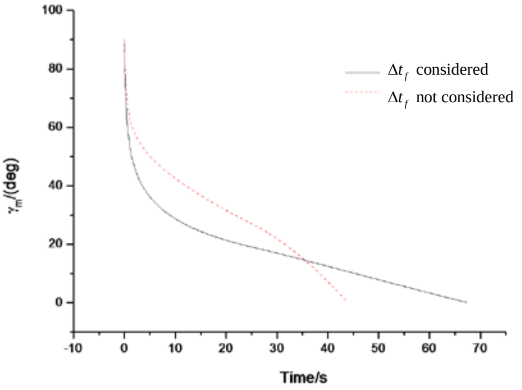

Figure 3. Flight path angle curve.

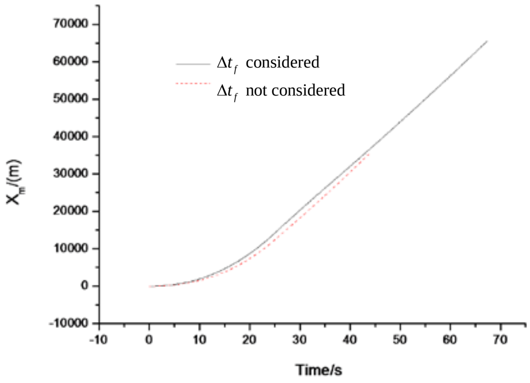

Figure 4. Displacement X change curve.

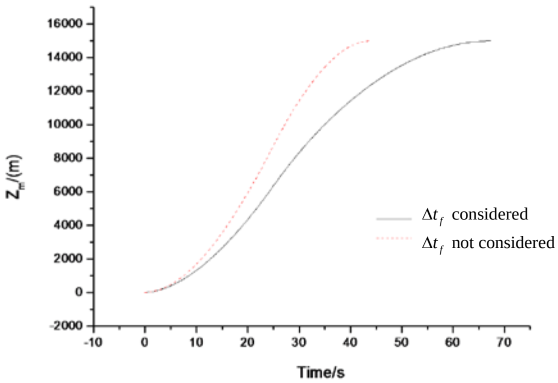

Figure 5. Displacement Z change curve.

5. Conclusion

This paper improves the MPSP guidance method, considers the time deviation of the end time, and deduces the MPSP guidance method with free end time. It has good application value and development prospect. MPSP guidance method transforms the dynamic optimization problem into a static optimization problem, and the updated control quantity is in the form of closed loop. Because the sensitivity matrix is calculated by recursion, this method has high computational efficiency. MPSP guidance method is used to plan the trajectory of ballistic missile in the powered phase. It can adjust the shape of the trajectory and improve the autonomous penetration ability of the missile in the powered phase.

References

[1] Hongyu Zhou, Xiaogang Wang, Naigang Cui. (2019). Glide trajectory optimization for hypersonic vehicles via dynamic pressure control [J]. Acta Astronautica, 2019, 164.

[2] Haibo Ji, LeiWang. (2019). Trajectory Tracking Strategy for Gliding Hypersonic Vehicle with Aileron Stuck at an Unknown Angle [J]. Journal of Beijing Institute of Technology, 2019, 28(03): 447-455.

[3] Zhao Jisong, Zhang Jianhong, Li Shuang. (2019). Rapid and High-Accuracy Approach for Hypersonic Glide Vehicle Reentry Trajectory Optimization [J]. Journal of Astronautics, 2019, 40(09): 1034-1043.

[4] Yao Zhang, Xiao Wang, Shengjing Tang. (2019). A globally fixed-time solution of distributed formation control for multiple hypersonic gliding vehicles [J]. Aerospace Science and Technology, 2019.

[5] Kun Zhao, DengQing Cao, WenHu Huang. (2018). Maneuver control of the hypersonic gliding vehicle with a scissored pair of control moment gyros [J]. Science China Technological Sciences, 2018, 61(8).

[6] Jianwen Zhu, Ruizhi He, Guojian Tang,Weimin Bao. (2018). Pendulum maneuvering strategy for hypersonic glide vehicles [J]. Elsevier Masson SAS, 2018, 78.

[7] Oza, H. B. and Padhi, R. (2012). Impact-Angle-Constrained suboptimal model predictive static programming guidance of air-to-ground missiles [J]. Journal of Guidance, Control, and Dynamics, 2012, 35(1): 153-164.

[8] Arnab Maity, Harshal B., Oza and Radhakant Padhi. (2013). Generalized model predictive static programming and its application to 3D impact angle constrained guidance of Air-to-Surface missiles [C]. 2013 American Control Conference (ACC), Washington, DC, USA, 2013: 4999-5014.